JOURNAL OF SOLID STATE CHEMISTRY 22, 353–360 (1977)

# Itinerant Electron Ferromagnetism in $Sr^{2+}$-, $Ca^{2+}$-, and $Ba^{2+}$-Doped Rare-Earth Orthocobaltites ($Ln^{3+}_{1-x}M^{2+}_{x}CoO_3$)†

C. N. R. RAO*

*Solid State and Structural Chemistry Unit, Indian Institute of Science, Bangalore 560012, India*

OM PARKASH, D. BAHADUR, P. GANGULY

*Programme in Materials Science and Department of Chemistry, Indian Institute of Technology, Kanpur 208016, India*

AND S. NAGABHUSHANA

*National Aeronautical Laboratory, Bangalore 560017, India*

Received March 29, 1977; in revised form May 20, 1977

Electronic and magnetic properties of $Ln_{1-x}Sr_xCoO_3$ ($Ln$ = Pr, Nd, Sm, Eu, and Gd) systems show that above a critical value of $x$, the $d$ electrons become itinerant while the materials become ferromagnetic at low temperatures. The ferromagnetic component increases with increase in $x$ and decrease in temperature. The Curie temperature increases with $x$ and decreases with decrease in the size of the rare-earth ion. Incorporation of $Ba^{2+}$ in $LaCoO_3$ favors itinerant electron ferromagnetism relative to $Sr^{2+}$ while $Ca^{2+}$ is less favorable than $Sr^{2+}$.

## 1. Introduction

Detailed investigations of lanthanum orthocobaltite, $LaCoO_3$, have shown that cobalt ions in this oxide have the diamagnetic, low-spin configuration ($t_{2g}^6$) at very low temperatures (*1*, *2*). With increase in temperature, the low-spin cobalt ions transform to the paramagnetic, high-spin state ($t_{2g}^4e_g^2$) and the inverse magnetic susceptibility versus temperature curve shows a plateau in the 400–650°K region due to short-range ordering of the two-spin states. Beyond this region, a symmetry change from $R\bar{3}c$ to $R\bar{3}$ has been noticed. With further increase in temperature, there is electron transfer from the high-spin cobalt ions to the low-spin ions, giving rise to intermediate charge-transfer states like $Co^{4+}$, $Co^{2+}$, and so on. Around 1200°K, $LaCoO_3$ exhibits a first-order transition due to the delocalization of the $e_g$ electrons (localized on $Co^{3+}$ ions at low temperatures) forming a $\sigma^*$ band state. Beyond 1200°K, $LaCoO_3$ becomes metallic. Mössbauer studies (*2*) have provided information on the nature of the spin- and valence-state equilibria of cobalt ions. While at low temperatures, Mössbauer spectra show unique resonances due to different cobalt states, only a single resonance corresponding

* To whom all correspondence should be addressed.

† Communication No. 4 from the Solid State and Structural Chemistry Unit.





ISSN 0022–4596

to the band state is seen above the localized ⇌ itinerant electron transition around 1200°K.

Substitution of $La^{3+}$ in $LaCoO_3$ by $Sr^{2+}$ (creating $Co^{4+}$ holes) brings about remarkable changes (*3–5*). Thus, the system $La_{1-x}Sr_xCoO_3$ becomes ferromagnetic at low temperatures when $x > 0.125$, the ferromagnetism arising from the positive $Co^{4+}$–O–$Co^{3+}$ interaction; the *d* electrons show itinerant behavior (both above and below $T_c$) in these compositions. The composition $La_{0.5}Sr_{0.5}CoO_3$ is a metallic ferromagnet ($T_c$ = 232°K) with a brown bronze luster. Another novel feature of $La_{1-x}Sr_xCoO_3$ ($x > 0.125$) is that the ferromagnetic $Sr^{2+}$-rich clusters coexist with the paramagnetic $La^{3+}$-rich regions in the same crystallographic phase, with the ferromagnetic component increasing with increasing $x$ and decreasing temperature. This interesting itinerant-electron ferromagnetic behavior of $La_{1-x}Sr_xCoO_3$ has prompted us to investigate electron transport, magnetic, and related properties of similar systems formed by other rare earths. It is noteworthy that electronic and magnetic properties of the lighter rare-earth orthocobaltites (*6*, *7*), $LnCoO_3$ (*Ln* = Pr to Gd), are essentially similar to those of $LaCoO_3$. In addition to the various $Ln_{1-x}Sr_xCoO_3$ systems (*Ln* = Pr, Nd, Sm, Eu, and Gd), we have studied some of the analogous $Ln_{1-x}Ca_xCoO_3$ and $La_{1-x}Ba_xCoO_3$ systems for the purpose of studying the effect of size of the divalent cation on the magnetic and electrical properties. It was considered worthwhile to find out whether the rare-earth ion contributes to the ferromagnetic behavior of these divalent cation-doped rare-earth orthocobaltites where the rare-earth ion has a magnetic moment. Our interest in $Ln_{1-x}Sr_xCoO_3$ and related materials was further strengthened by the applications found for such materials in fuel cells (*8*).

## 2. Experimental

All the $Ln_{1-x}Sr_xCoO_3$ samples (*Ln* = Pr, Nd, Sm, Eu, and Gd) with $0 \leqslant x \leqslant 0.5$ were prepared by the decomposition of the appropriate mixtures of oxalates. The resulting solids were repeatedly ground, pressed as pellets, and heated at 1400–1500°K for several hours. X-ray diffraction patterns were taken at each stage to monitor the completion of the reaction. The final products were pressed into pellets and sintered again at 1300°K to form hard, dense bars. The bars were of high density, particularly in the nearly metallic or metallic samples ($x > 0.2$). In the case of $Ln_{1-x}Ca_xCoO_3$ (La, Sm, and Gd), we could prepare compositions only up to $x = 0.3$ in the case of La and up to 0.2 in the case of Sm and Gd. In $Ln_{1-x}Ba_xCoO_3$, only compositions up to $x = 0.1$ were prepared.

Electrical resistivity (employing the four-probe method) as well as Seebeck-coefficient measurements were made in the temperature range 300–1000°K. Magnetic susceptibility measurements were made in the range 140–800°K employing locally built apparatus. Mössbauer spectra were recorded employing a home-built constant-velocity spectrometer. Hysteresis measurements were made at 77°K employing a pulsed magnetic field with an apparatus constructed at the National Aeronautical Laboratory.

## 3. Results and Discussion

$LaCoO_3$ is a perovskite with rhombohedral distortion with the $La^{3+}$ ion occupying the *A* site. Substitution of $Sr^{2+}$ for $La^{3+}$ in $La_{1-x}Sr_xCoO_3$ creates $Co^{4+}$ holes without any appreciable formation of oxygen ion vacancies up to a value of $x = 0.5$. When $x > 0.5$, the concentration of oxygen ion vacancies becomes appreciable (*3*). Variation of lattice parameters of $La_{1-x}Sr_xCoO_3$ with $x$ has been reported by Raccah and Goodenough (*4*) and also by Bhide *et al.* (*5*). The rhombohedral distortion decreases with increasing $x$ and finally, the composition $La_{0.5}Sr_{0.5}CoO_3$ is cubic; electron diffraction studies (*9*) of $La_{0.5}Sr_{0.5}CoO_3$ show evidence for the formation of superstructure corresponding to doubling of the unit cell ($a = 5.385$ Å). Behavior of $Pr_{1-x}Sr_xCoO_3$ is similar to that of

$LaCoO_3$ with a cubic phase when $x = 0.5$ ($a = 5.382$ Å). However, as the radius of the rare-earth ion decreases further, the nature of distortion in the parent cobaltite, $LnCoO_3$, changes (*10*). Thus, $NdCoO_3$ is essentially tetragonal while $GdCoO_3$ is orthorhombic. In $Nd_{1-x}Sr_xCoO_3$ the tetragonal distortion decreases with increase in $Sr^{2+}$ concentration and $Nd_{0.5}Sr_{0.5}CoO_3$ can be indexed essentially as a cubic structure ($a = 5.387$ Å). As we go down the rare-earth series, the tolerance factor for the perovskite structure of $Ln_{1-x}Sr_xCoO_3$ appears to become smaller as noticed by Ohbayashi *et al.* (*11*). Perovskite-type $Ln_{1-x}Sr_xCoO_3$ solids seem to be formed for all values of $x$ ($0 < x < 0.6$) only up to Gd (Fig. 1). In a system like $Er_{1-x}Sr_xCoO_3$, the perovskite structure is obtained only when $x = 0.5$. The distortions found in $Ln_{1-x}Sr_xCoO_3$ systems ($Ln$ = Nd to Gd) vary from tetragonal to orthorhombic or monoclinic. We have restricted our studies only to the perovskite type of $Ln_{1-x}Sr_xCoO_3$ solids (Fig. 1). We have not indexed the X-ray patterns of all the samples in detail to get the exact unit-cell dimensions, but we have ensured the formation of these compounds by repeated heating and quenching followed by examination of X-ray diffraction patterns. The lattice dimensions are not greatly affected up

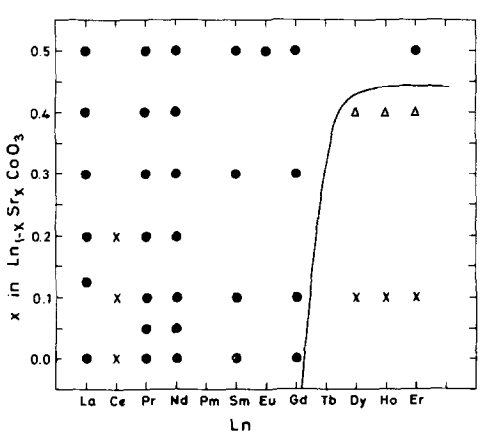


FIG. 1. Region of perovskite formation in $Ln_{1-x}Sr_xCoO_3$: closed circles, perovskite structure; triangles, perovskite formed with other structures (after Ref. (*11*)); crosses, other structures only (after Ref. (*11*)).

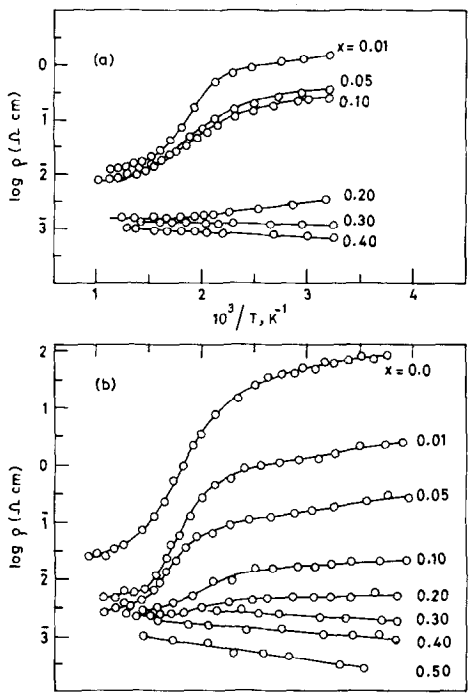


FIG. 2. Plot of logarithm of resistivity against reciprocal of temperature in $Ln_{1-x}Sr_xCoO_3$: (a) Pr, (b) Nd.

to $x = 0.3$. The pseudocubic lattice parameters of $Ln_{0.5}Sr_{0.5}CoO_3$ compositions, however, show a gradual decrease from La to Gd. Substitution for $Ca^{2+}$ for $Ln^{3+}$ in $LnCoO_3$ ($Ln$ = La, Sm, or Gd) does not affect the perovskite structure of the parent orthocobaltite. The lattice dimensions are only slightly affected up to $x = 0.3$ just as in the case of $Sr^{2+}$.

Electrical resistivity data of two typical $Ln_{1-x}Sr_xCoO_3$ systems ($Ln$ = Pr, Nd) are shown for different values of $x$ in Fig. 2. We clearly see that the resistivity progressively decreases with increase in $x$, the system becoming metallic when $x \geqslant 0.3$. Thus, in all these systems, a semiconductor–metal transition occurs as the concentration of $Sr^{2+}$ (or $Co^{4+}$ holes) is increased. Seebeck coefficients, $\alpha$, also show evidence for this behavior (Fig. 3). When $x$ is small, $\alpha$ decreases markedly with increase in temperature at first and then decreases gradually with further increase in temperature. At large $x$, when the system is

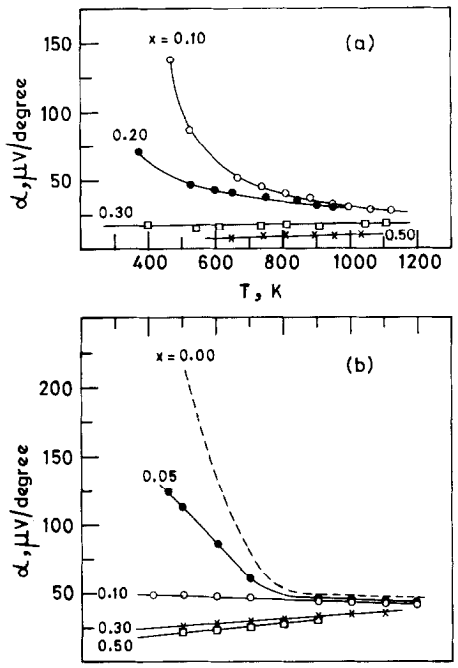


FIG. 3. Plot of Seebeck coefficient against temperature in $Ln_{1-x}Sr_xCoO_3$: (a) Pr, (b) Nd.

metallic, $\alpha$–$T$ curves show a slight positive slope. Thus, electron transport properties of all the $Ln_{1-x}Sr_xCoO_3$ systems studied by us indicate that the $d$ electrons become itinerant above a critical concentration of $Sr^{2+}$. This can be visualized from Fig. 4 where we have plotted the Seebeck coefficient against $x$. In

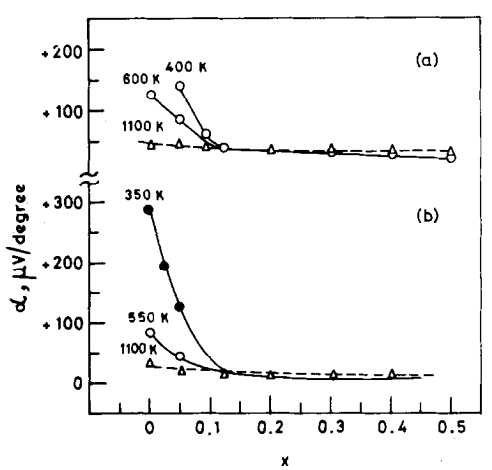


FIG. 4. Plot of Seebeck coefficient against $x$ in $Ln_{1-x}Sr_xCoO_3$: (a) Nd, (b) La.

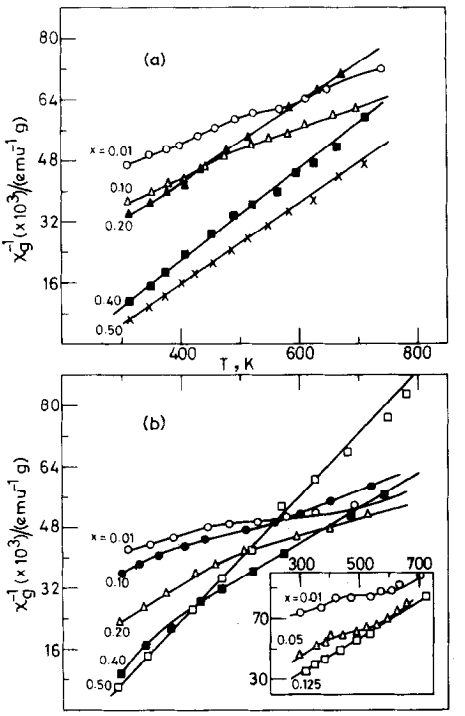


FIG. 5. Inverse susceptibility–temperature plots of $Ln_{1-x}Sr_xCoO_3$: (a) Pr, (b) Nd. Data below 300°K are not shown. In the inset, data for a few compositions of $La_{1-x}Sr_xCoO_3$ are shown.

$La_{1-x}Sr_xCoO_3$ and $Nd_{1-x}Sr_xCoO_3$, the critical value of $x$ is between 0.1 and 0.15. It is only above this critical composition that these oxides exhibit ferromagnetism at low temperatures.

Plots of inverse magnetic susceptibilities, $\chi^{-1}$, against temperature for two typical $Ln_{1-x}Sr_xCoO_3$ systems ($Ln$ = Pr and Nd) are shown in Fig. 5. In the inset of the figure, inverse susceptibility–temperature plots of a few compositions of $La_{1-x}Sr_xCoO_3$ are also shown. The data clearly show that when $x$ is small, the susceptibility behavior is somewhat similar to that of the parent orthocobaltites (*2*, *5–7*), with a plateau in the 400–650°K region. When $x$ is above the critical concentration (0.1 to 0.15), $\chi^{-1}$ — $T$ plots clearly show ferromagnetic behavior with positive values of the paramagnetic Curie temperatures, $\theta_p$, just as in the case of $La_{1-x}Sr_xCoO_3$. The values of $\theta_p$ for various $Ln_{1-x}Sr_xCoO_3$ systems are

TABLE I

CURIE TEMPERATURES IN $Ln_{1-x}Sr_xCoO_3$[a]

| | Value of $x$ | | | | |
|---|---|---|---|---|---|
| *Ln* | 0.10 | 0.20 | 0.30 | 0.40 | 0.50 |
| La | 70[b] (30)[c] | 180[b] (100)[c] | 265 (150)[c] | 312[b] (200)[c] | 316 (232)[c] |
| Pr | −125 | — | — | 225 | 250 |
| Nd | −220 | 65 | — | 135 (90 ± 10) | 260 (190 ± 15) |
| Sm | 45 | — | 60 | — | 190 (160 ± 10) |
| Eu | — | — | — | — | 150 |
| Gd | 5 | — | 40 | — | 100 (90 ± 10) |

[a] Values in parentheses are $T_c$ values.
[b] From Ref. (*3*).
[c] $T_c$ values from Ref. (*4*).

tabulated in Table I. The values of $\theta_p$ found by us in case $La_{1-x}Sr_xCoO_3$ are close to those reported by Jonker and Van Santen (*3*). We see that $\theta_p$ values in all the systems is positive when $0.1 \leqslant x < 0.5$, the systems becoming increasingly ferromagnetic with increasing $x$ in this range.

Ferromagnetic Curie temperatures for a few of the compositions of $Ln_{1-x}Sr_xCoO_3$ are also shown in Table I. While both $\theta_p$ and $T_c$ increase in $x$ in all the $Ln_{1-x}Sr_xCoO_3$ systems studied, the values decrease down the rare-earth series accompanying the decrease in the size of the rare-earth ion. The increasing trend of $\theta_p$ and $T_c$ with increase in $x$ probably results from the variation in the band occupancies; in addition, there would be increased 180° interaction since the system becomes closer to the ideal perovskite structure with increase in $x$. We should note that the ferromagnetic component in these oxide systems also increases with $x$. The observed decrease in $\theta_p$ and $T_c$ values down the rare-earth series could arise from the decreased 180° interaction, which in turn is related to differences in structure of these distorted perovskites (*10*).

We have studied magnetic hysteresis in $Ln_{0.5}Sr_{0.5}CoO_3$ ($Ln$ = La, Pr, Nd, Sm, and

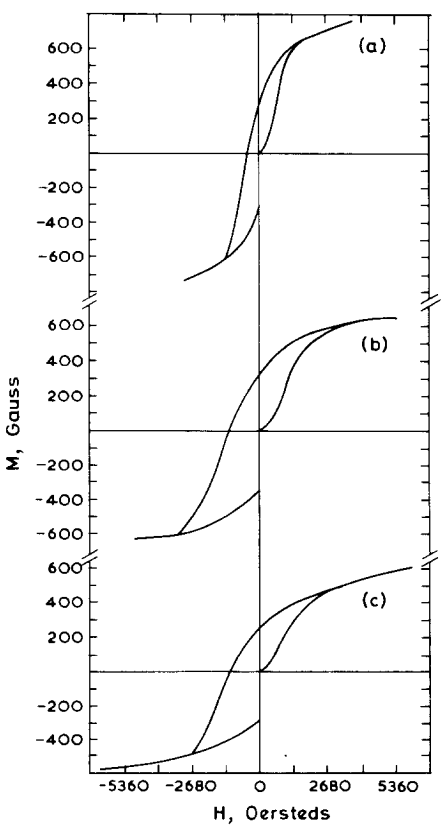


FIG. 6. Magnetization curves in $Ln_{1-x}Sr_xCoO_3$ at 77°K: (a) Pr, (b) Nd, (c) Gd.

TABLE II

MAGNETIC HYSTERESIS DATA OF $Ln_{0.5}Sr_{0.5}CoO_3$

| *Ln* | Remnant magnetization (G) | Coercive field (G) |
|---|---|---|
| La | 110 | 400 |
| Pr | 275 | 470 |
| Nd | 340 | 1275 |
| Sm | 260 | 1200 |
| Gd | 200 | 670 |

Gd) at 77°K and typical hysteresis loops are shown in Fig. 6. An interesting feature in many of these samples is the absence of saturation at high fields; a similar observation was made earlier by Menyuk *et al.* (*12*) in the case of $La_{0.5}Sr_{0.5}CoO_3$. Results from hysteresis curves are shown in Table II. The hysteresis data along with the results from susceptibility measurements show that the ferromagnetism is entirely due to cobalt ions and that the rare-earth ions do not participate in any way in the magnetic ordering.

Magnetic moments, $\mu_{eff}$/cobalt ion, were calculated employing the equation,

$$\mu_{eff} = 2.84(\chi_M(T - \theta_p))^{1/2}\beta$$

where $\chi_M$ is the molar susceptibility and $T$ is the absolute temperature. In all the systems studied, $\mu_{eff}$ calculated by this relation (after subtracting the contribution for the rare-earth ion, where needed) is between 1.3 and 2.8 (a value much smaller than that expected for high-spin $Co^{3+}$ or $Co^{4+}$ ions) at 300°K for all the compositions of $Ln_{1-x}Sr_xCoO_3$ ($x > 0.1$, $Ln$ = Pr, Nd, Sm, Eu, or Gd). The values of $\mu_{eff}$ in the case of $La_{1-x}Sr_xCoO_3$ obtained by us are close to those reported by Jonker and Van Santen (*3*). We have also estimated $\mu_{eff}$ values from magnetization data of $Ln_{0.5}Sr_{0.5}CoO_3$ ($Ln$ = Pr, Nd, and Sm). The $\mu_B$ thus found is about 1.5 per cobalt ion just as in the case of $La_{0.5}Sr_{0.5}CoO_3$ (*4*), although there is small uncertainty in the estimate due to absence of saturation.

Magnetic and transport properties of various $Ln_{1-x}Sr_xCoO_3$ systems discussed hitherto clearly show that in all these systems, *d* electrons become itinerant and the materials become ferromagnetic (at low temperatures) above a critical value of $x$. The link between the ferromagnetism at low temperatures and itinerancy of *d* electrons in $La_{1-x}Sr_xCoO_3$ was established by Bhide *et al.* (*5*) by studying $^{57}Co$ Mössbauer spectra. These workers found unique Mössbauer resonances due to different cobalt states (at 300°K) only when $x$ was below the critical concentration of 0.125. Above this critical concentration a single Mössbauer resonance due to a time-averaged electronic configuration of cobalt ions was found indicating impurity band formation. Only those compositions where there was impurity band formation at 300°K exhibited ferromagnetic hyperfine structure in the Mössbauer spectra at low temperatures. In order to ascertain that the same situation holds in other $Ln_{1-x}Sr_xCoO_3$ systems, we examined the Mössbauer spectra of $Nd_{1-x}Sr_xCoO_3$ and found the results to be similar to those in $La_{1-x}Sr_xCoO_3$. The internal field in $Nd_{0.7}Sr_{0.3}CoO_3$ ($x > 0.1$) estimated from Mössbauer hyperfine structure is 160 kOe, a value somewhat lower than in $La_{0.7}Sr_{0.3}CoO_3$.

The observation of a ferromagnetic moment of about $1.5\mu_B$ per cobalt ion in $Ln_{0.5}Sr_{0.5}CoO_3$ can be interpreted in terms of the overlapping $\sigma^*$ band of up-spin and $\pi^*$ band of down-spin (*4*). As long as the $\sigma^*$ band remains less than one-quarter filled and the $\pi^*$ band more than three-quarter filled, itinerant-electron ferromagnetism having a Weiss constant $\theta > T_c$ is expected. The spin contribution to the average cobalt ion moment is given by $\mu_{Co} = (x + 2n)\mu_B$, where $n$ is the number of electrons in the $\sigma^*$ orbital, $n$ increasing in a complex way with $x$. An effective magnetic moment of $1.5\mu_B$/Co ion gives a value of $n = 0.5$ for the number of up-spin $\sigma^*$ electrons per molecule in $Ln_{0.5}Sr_{0.5}CoO_3$. Such a band picture explains the observed transport and magnetic properties fairly satisfactorily as discussed elsewhere by Raccah and Goodenough (*4*) as well as Bhide *et al.* (*5*). The fact that $\mu_{Co} \approx 1.5\mu_B$ also indicates the presence of $x + n = 1$ holes per molecule in the

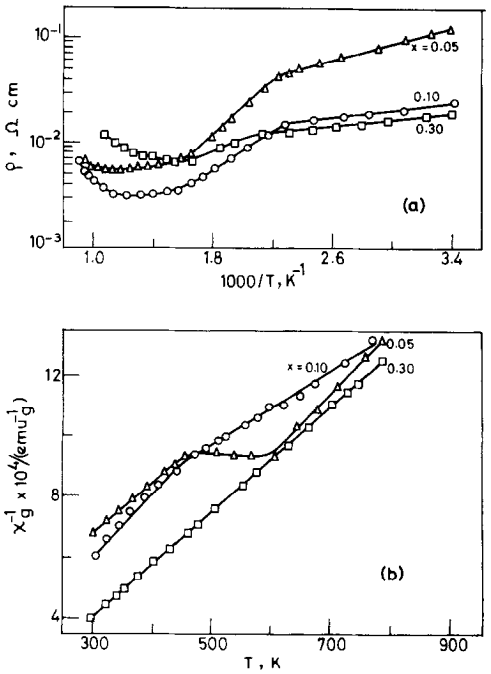


FIG. 7. (a) Resistivity and (b) magnetic susceptibility data of $La_{1-x}Ca_xCoO_3$.

$\pi^*$ band. This suggests electron correlation splitting of the $\pi^{*5}$ and $\pi^{*6}$ manifolds (as to be anticipated for narrow $\pi^*$ bands). In such a case, the Fermi energy would lie between the two $\pi^*$ bands in a partially filled overlapping $\sigma^*$ band (*5*, *13*). However, the continued increase in magnetization with very high fields implies that the number $n$ of $\sigma^*$ band electrons per cobalt atom is a function of $H$ as well as of $x$. We may conclude that at $x = 0.5$, the Fermi energy has just passed to (or through) the top of the $\pi^{*5}$ configuration.

In order to study the effect of the divalent ion, $M^{2+}$, in $Ln^{3+}_{1-x}M^{2+}_xCoO_3$ on the properties, we have examined calcium- and barium-doped samples. Resistivity and magnetic susceptibility data of few compositions of $La_{1-x}Ca_xCoO_3$ are shown in Fig. 7. We see that the behavior is quite similar to the $Sr^{2+}$-doped materials although the effect of $Ca^{2+}$ in bringing out itinerant properties seems to be slightly less than the $Sr^{2+}$. Thus, the sample with $x = 0.3$ is distinctly a semiconductor in the $Ca^{2+}$ system with appreciable activation energy, while in the $Sr^{2+}$ system the activation energy for conduction is close to zero. The $\theta_p$ values of $Ca^{2+}$-doped samples is much lower than those of $Sr^{2+}$-doped samples. Thus, the values of $\theta_p$ in $La^{3+}_{1-x}M^{2+}_xCoO_3$ for $x = 0.3$ are 265 and 50°K, respectively, for $Sr^{2+}$ and $Ca^{2+}$. In the corresponding Gd system ($x = 0.2$), $\theta_p = -35$°K for $Ca^{2+}$ while it is +25°K for $Sr^{2+}$. This is understandable because the smaller $Ca^{2+}$ ion in the $A$ site does not favor 180° interaction compared to the larger $Sr^{2+}$ ion. The value of $\mu_{eff}$/Co ion is between 1.3 and 2.5 in the systems studied, not different from the values encountered in the analogous $Sr^{2+}$ systems.

In $La_{1-x}Ba_xCoO_3$, the $Ba^{2+}$ ion by virtue of its larger size shows more drastic effects on the electronic and magnetic properties. Thus, the sample with $x = 0.1$ shows only a small temperature dependence of resistivity and almost becomes metallic above 700°K. The $x = 0.1$ sample is ferromagnetic at low temperatures with a $\theta_p$ of 100°K; this $\theta_p$ value is higher than that in the corresponding composition of the $Sr^{2+}$- or $Ca^{2+}$-doped system.

## Acknowledgment

The authors thank Mr. V. S. Ganesh for his assistance in making the hysteresis measurements.

## References

1. P. M. RACCAH AND J. B. GOODENOUGH, *Phys. Rev.* **155**, 932 (1967).
2. V. G. BHIDE, D. S. RAJORIA, G. RAMA RAO, AND C. N. R. RAO, *Phys. Rev. B* **6**, 1021 (1972).
3. G. H. JONKER AND J. H. VAN SANTEN, *Physica* **19**, 120 (1953).
4. P. M. RACCAH AND J. B. GOODENOUGH, *J. Appl. Phys.* **39**, 1209 (1968).
5. V. G. BHIDE, D. S. RAJORIA, C. N. R, RAO, G. RAMA RAO, AND V. G. JADHAO, *Phys. Rev. B* **12**, 2832 (1975).
6. D. S. RAJORIA, V, G. BHIDE, G. RAMA RAO, AND C. N. R. RAO, *J. Chem. Soc. Faraday II* **70**, 512 (1974)
7. V. G. JADHAO, R. M. SINGRU, G. N. RAO, D. BAHADUR, AND C. N. R. RAO, *J. Phys. Chem. Solids* **37**, 113 (1976), and other references listed therein.

*8.* C. S. TEDMON JR., H. S. SPACIL, AND S. P. MITOFF, *J. Electrochem. Soc.* **116**, 1170 (1969).
*9.* P. L. GAI AND C. N. R. RAO, *Mater. Res. Bull.* **10**, 787 (1975).
*10.* G. DENAZEAU, M. POUCHARD, AND P. HAGENMULLER, *J. Solid State Chem.* **9**, 202 (1974).
*11.* H. OHBAYASHI, T. KUDO, AND T. GEJI, *Jpn. J. Ap Phys.* **13**, 1 (1974).
*12.* N. MENYUK, P. M. RACCAH, AND K. DWIGHT, *Ph Rev.* **166**, 510 (1968).
*13.* J. B. GOODENOUGH, *Mater. Res. Bull.* **6**, 9 (1971).